

Efficient inverted hybrid solar cells using both CuO and P3HT as an electron donor materials

M. Ikram^{1,3,4}  · M. Imran² · J. M. Nunzi^{3,4} · S. Ali¹

Received: 24 January 2015 / Accepted: 22 May 2015 / Published online: 30 May 2015
© Springer Science+Business Media New York 2015

Abstract Copper oxide (CuO) nanoparticles (<50 nm) were incorporated in the P3HT—poly(3-hexylthiophene):PCBM-[6,6]—phenyl-C61-butyric acid methyl ester bulk heterojunction organic solar cells. The ratio of P3HT to CuO in the blend was varied, while maintaining the fixed ratio of PCBM. The addition of CuO nanoparticles was found to significantly improve the power conversion efficiency in the P3HT:PCBM solar cells under AM 1.5 G and 100 mW/cm² irradiation. The mixing of CuO in the active layer widens the light absorption range and introduced a red shift in the absorption spectra. The CuO-conjugated active layer increased the surface roughness. The CuO nanoparticles agglomerated in the blend as their concentration relative to P3HT increased in the active layer.

1 Introduction

So far, studies on organic–inorganic hybrid solar cells were mostly based on binary systems. Researches on ternary systems which are consists of polymers, PCBM and

nanocrystals are rarely reported [1, 2]. Chin et al. [3] increased short circuit current density (J_{sc}) by incorporating gold (Au) nanocrystals in a P3HT:PCBM system. Ternary blend solar cells are simple and efficient technique to improving the device performance [4–6]. J_{sc} can be easily enhanced in ternary blend solar cells by adding a light-harvesting 3rd material with an absorption band matching to P3HT:PCBM binary blends [7–11]. Recently, organic solar cells fabricated using ternary blends of P3HT, silicon phthalocyanine bis(trihexylsilyl oxide) (SiPc) and PCBM. Because SiPc has absorption band in the near-infrared region, J_{sc} was significantly improved in the P3HT:PCBM:SiPc ternary blend system [4–8].

Moreover, we have reported hybrid organic solar cells based on ternary blends of P3HT:PCBM:TiO₂ and P3HT:PCBM:ZnO. J_{sc} was effectively increased due to absorption of nanoparticles in the UV-region and formed percolation network in the active layer of the ternary blend solar cells [12, 13]. Moreover, we have demonstrated that J_{sc} is further improved in quaternary blend solar cells based on P3HT, PCBM, ZnO, and TiO₂ nanoparticles [5].

Oxide semiconductors CuO, NiO and Cu₂O are alternatives to conjugated polymer in organic solar cells. The CuO is potential candidate materials due to higher optical absorption, low cost of raw materials and non-toxic. CuO has band gap energies of 1.5 eV, which is very close to the ideal energy gap of 1.4 eV for solar cells and allows for good solar spectral absorption [14].

In hybrid devices normally use a conventional architecture where bulk heterojunction active layer is sandwiched between low work function (Al) for electron collecting cathode and high work function transparent conducting oxide (ITO) as hole collecting anode after passing through a buffer layer of poly(3,4-

✉ M. Ikram
mianraj.1981@gmail.com

¹ Solar Cell Applications Research Lab, Department of Physics, Government College University, Lahore 54000, Punjab, Pakistan

² Technical Institute of Physics and Chemistry, Chinese Academy of Sciences, 29 Zhongguancun East Road, Haidian District, Beijing 100190, China

³ Department of Physics, Queen's University, Kingston, ON K7L 3N6, Canada

⁴ Department of Chemistry, Queen's University, Kingston, ON K7L 3N6, Canada

ethylenedioxythiophene):poly(styrenesulfonate) (PEDOT:PSS). However, the interface between the acidic anodic buffer layer PEDOT:PSS and a common transparent electrode such as ITO has been proven unstable in air, especially under humid conditions [15]. Another issue with these devices is oxidation of low work function electrode as prolonged exposure in air and degradation of the photoactive layer. Alternatively, an inverted configuration can improve the life time by using a high work function (Au, Ag, Pt) electrode and a buffer layer of ZnO underneath the active layer to support collect electrons and depositing PEDOT:PSS or MoO₃ as a hole transport layer on active layer. Due to these buffer layers in inverted architecture prevent shorting and reduce leakage current in hybrid devices. The oxidation of low work function metal can also help reduce by using high work function metal (Au, Ag or Pt) as top contact, effectively reversing the polarity of the device [16].

In this work, ternary system hybrid solar cells containing of CuO nanoparticles, P3HT and PCBM with an inverted structure were fabricated. When CuO is mixed in the active layer of BHJ devices, it can enhance the light harvesting zone and reduce the cost of solar cells. Therefore, we fabricated the devices with a P3HT:CuO:PCBM blend. The incorporation of CuO in the polymer blend (P3HT:PCBM) is considered in this study. From a detailed balance analysis, CuO with a band gap of 1.4 eV can reach an ultimate solar cell efficiency of almost 30 % [17]. The devices were fully characterized and the effect of the incorporation of CuO nanoparticles was discussed.

2 Experimental details

2.1 Materials

Indium tin oxide (ITO) coated glass substrates with sheet resistance of (20–25 Ω/sq.) were purchased from Lumtec, Taiwan. CuO nanoparticles <50 nm were purchased from Sigma-Aldrich. Highly regioregular P3HT (P200) and PCBM were obtained from Rieke Metals and SES, USA respectively. All the materials were used without further purification.

2.2 Device fabrication

The ITO coated glass substrates were etched using 10 vol% hydrochloric acid to generate an insulated area to avoid short circuiting. The etched slides were cleaned prior to use by ultrasonic agitation in a detergent solution, deionized water, acetone and isopropanol each for 5 min. The slides were dried using the stream of nitrogen and placed into plasma cleaner for 10 min.

2.2.1 Preparation of ZnO sol-gel

The ZnO film (electron transport layer) was prepared by mixing zinc acetate dihydrate (99.9 %, Sigma-Aldrich, 1 g) and ethanolamine (99.5 %, Sigma-Aldrich, 0.28 g) in 2-methoxyethanol (99.8 %, Sigma-Aldrich, 10 mL) under vigorous stirring for 12 h for the hydrolysis reaction in air [18]. Firstly, a buffer layer ZnO was spin coated at 3000 rpm for 40 s on ultrasonically cleaned ITO glass substrates. The samples were heated at fixed temperature (150 °C) for 1 h.

Ternary blends of P3HT:CuO:PCBM of various weight ratios (1:0:1, 0.75:0.25:1, 0.50:0.50:1, and 0.25:0.75:1) in 1 mL 1,2-di-chlorobenzene (DCB) were stirred for 12 h at 40 °C and passed through polytetrafluoroethylene (PTFE) syringe filter prior to using it to spin coat on the top of ZnO coated substrates. The spin coated films were sintered on the hotplate at 150 °C for 15 min in open air. Finally, a thin layer of MoO₃ (3 nm) and Ag (100 nm) film thickness were thermal evaporated with active device area of 0.2 cm². The devices structures were ITO/ZnO/(P3HT:CuO:PCBM/MoO₃/Ag as shown in Fig. 1.

2.3 Characterization

The current density–voltage (J–V) characterization was tested using a Keithley 2420 source meter with a solar simulator (CT 100 AAA) under AM 1.5 G with 100 mW/cm² irradiation intensity. EQE measurements were obtained in air using QEX 10 (PV Measurement) system. UV–Visible spectrophotometer (Lambda 35, Perkin Elmer) was used for absorption spectra measurements of the active layers. The active layers morphology was characterized by using atomic force microscope (AFM, Ambios technology, Q250).

3 Results and discussion

In Fig. 2 the graphs indicate the current density versus voltage (J–V) characteristics of fabricated devices with the ternary system (P3HT:CuO:PCBM) and the binary system

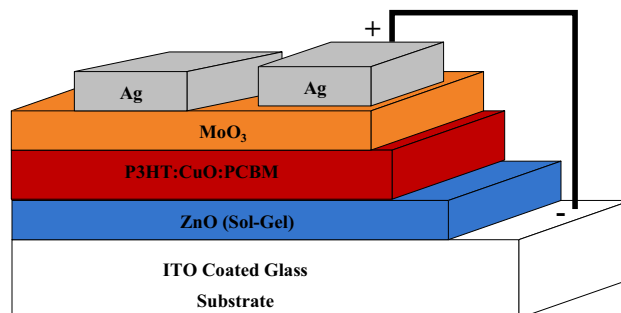


Fig. 1 The schematic representation of inverted hybrid BHJ devices based on CuO nanoparticles

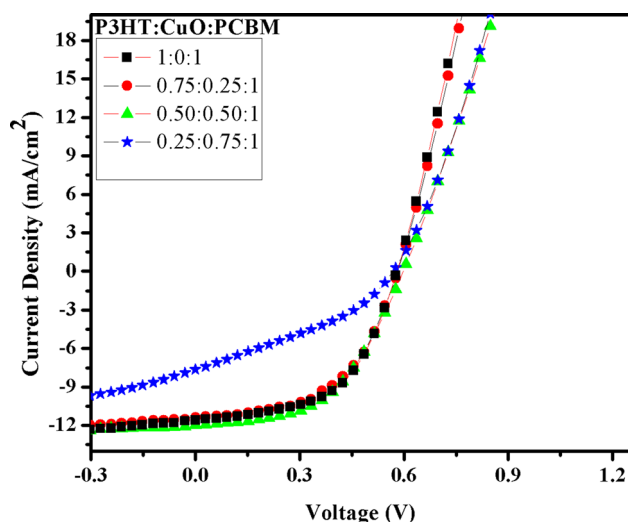


Fig. 2 J–V characteristics of various ratios of P3HT:CuO:PCBM devices

(P3HT:PCBM) were compared. Figure 2 indicates that the increase in efficiency with the incorporation of CuO nanoparticles in the active layer of the devices mainly originates from an increase in open circuit voltage (V_{oc}) and J_{sc} . We also see that an increase in R_s with increasing amount of CuO in the active layer of P3HT and PCBM where R_s was found from the curves based on the one-diode model. R_s was achieved to be approximately dV/dJ at large V .

Figure 3 shows the energy level diagram of inverted hybrid BHJ solar cells. Upon incidence of irradiation, both CuO nanoparticles and P3HT absorb photons and create excitons. The created excitons separate at the interface of donor–acceptor. In this structure the generated holes transport towards the MoO₃/Ag anode and electrons can either travel from P3HT to ZnO, P3HT to PCBM and P3HT to CuO. All these possible paths may increase charge generation in the active layer (Fig. 3).

The electron affinity LUMO level of CuO and PCBM are -4.1 and -4.4 eV, respectively [12, 19] so electron can also be transported from CuO to PCBM and finally collected by ITO electrode (-4.8 eV). It is believed that CuO:PCBM, P3HT:PCBM and P3HT:CuO interfaces enhance the charge separation and collection, resulting in a larger V_{oc} . The increase in J_{sc} with the addition of CuO in the active layer was attributed to the enhancement of light harvesting capability of CuO due to small band gap in solar cells. Hence, more photons were captured and more charges were produced [20]. The extracted values of the parameters are listed in Table 1.

From Table 1, the V_{oc} and J_{sc} increased with increasing amount of CuO nanoparticles in the blend. The resultant increase in efficiency reverses with high concentration of

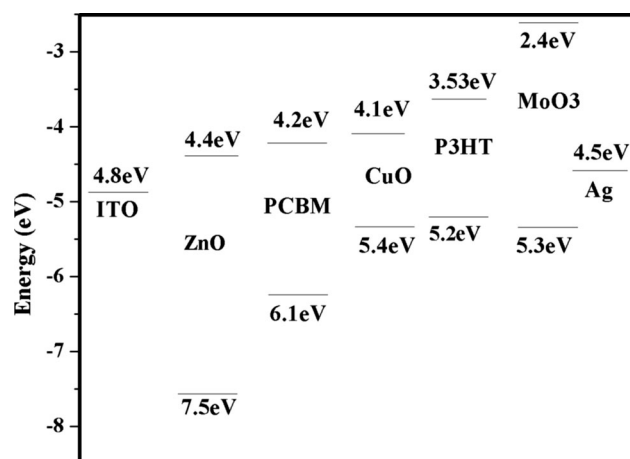


Fig. 3 Energy level diagram of CuO-conjugated inverted hybrid BHJ solar cells

CuO due to large scale aggregations of the CuO. The aggregates collapse the BHJ structure and remove the network for charge collection. As seen in Table 1, R_s increased from 9.1 to $16.5 \Omega\text{-cm}^2$ with increasing amount of CuO in the active layer. This increase in R_s reduced the FF of the devices resulted lower the PCE of 0.75:0.25:1.

Figure 4a–c display scanning electron microscope (SEM) images of the active layer of P3HT:CuO:PCBM with various ratios (1:0:1, 0.50:0.50:1 and 0.25:0.75:1) prepared in DCB. Figure 4a represents the surface morphology of the CuO free active layer (1:0:1). This active film is smoother than that CuO-doped polymer blend (b, c) with small and large clusters of PCBM. Figure 4b shows the image of the optimum amount (0.50:0.50:1) of CuO nanoparticles in the polymer blend were randomly dispersed and provides interconnected network to facilitate both electrons and holes in a continuous internal structure. Further addition of CuO in the polymer active layer (0.25:0.75:1) shows large agglomerates responsible for removing network for electrons and holes, as shown in Fig. 4c. To achieve high performing devices, it is essential to use a blend of both P3HT and CuO with PCBM.

The micro-morphologies of the active layers were performed with an atomic force microscope (AFM) to expose the effects from the incorporation of CuO nanoparticles. Figures 4c, and 5a show the surface topography of 1:0:1, 0.25:0.75:1 and 0.50:0.50:1 active layers respectively. Figure 5a indicates that the surface with no CuO (1:0:1) was relatively smooth with RMS roughness of 2.5 nm. Figure 5b, c represent that the surfaces are rough, with RMS roughness of 5.2 and 9.2 nm, respectively. The roughness of the films increased with increasing ratios of CuO nanoparticles in the active layer. The surface roughness of film was manifested to aggregation of CuO

Table 1 Photovoltaics parameters obtained for devices with binary and ternary system

Device structure	P3HT:CuO:PCBM	Voc (V)	Jsc (mA/cm ²)	FF (%)	Rs (Ω-cm ²)	PCE (%)
1:0:1		0.58	11.1	53.4	9.1	3.4 ± 0.2
0.75:0.25:1		0.58	11.4	52.9	13.9	3.5 ± 0.1
0.50:0.50:1		0.60	11.9	51.7	11.2	3.7 ± 0.3
0.25:0.75:1		0.57	7.7	35.2	16.5	1.5 ± 0.5

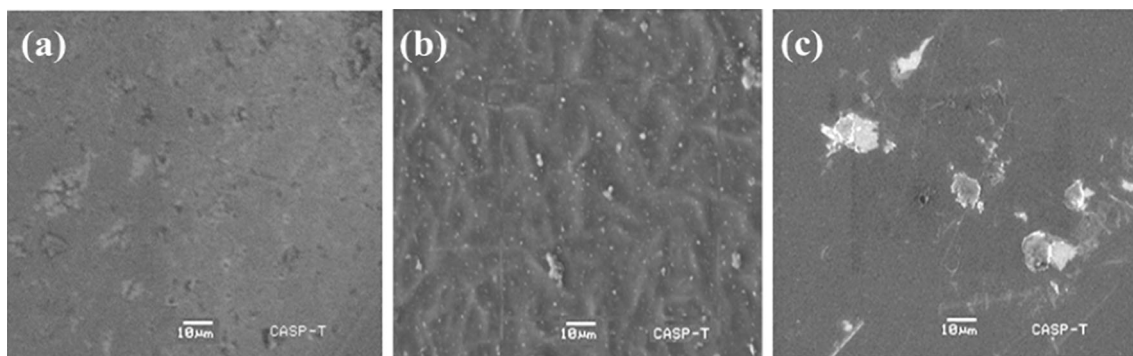
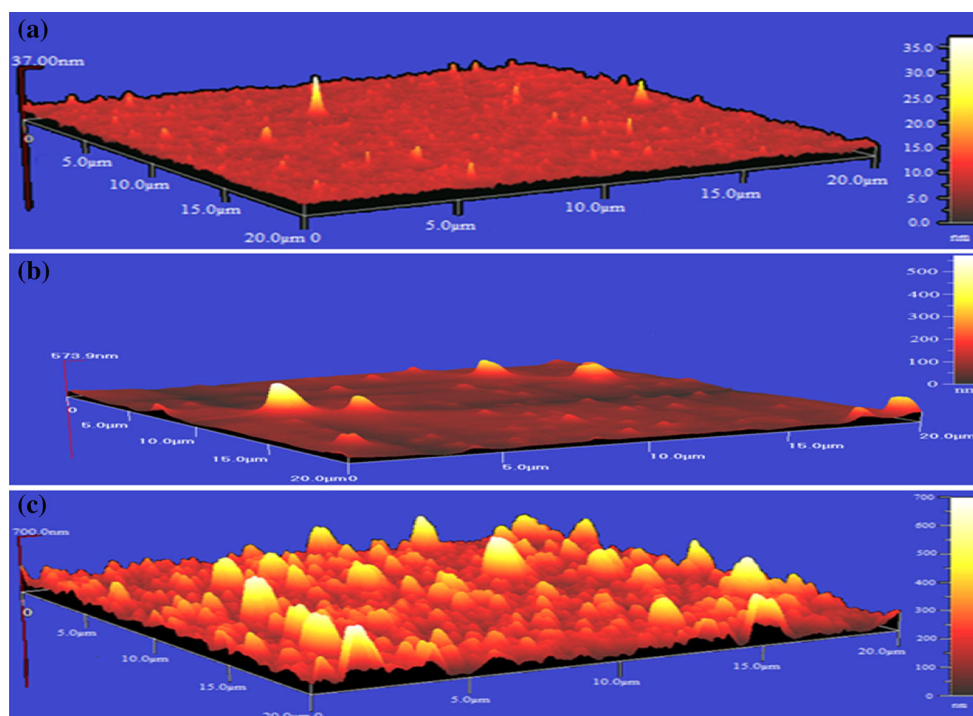


Fig. 4 SEM images of ratios 1:0:1, 0.50:0.50:1 and 0.25:0.75:1 (a–c) in DCB respectively

Fig. 5 AFM images of various ratios 1:0:1 (a), 0.75:0.25:1 (b) and 0.50:0.50:1 (c) of active layer



nanoparticles with increasing amount of CuO in the active layer blend.

Figure 6 depicts the UV–Vis absorption spectra of active layer films of binary and ternary system with various ratios were compared. Two peaks (330 and 490 nm) were found in the binary system corresponds to the absorption of PCBM and P3HT respectively. After the addition of CuO

nanoparticles, the absorption peak intensity reduced with increasing amount of CuO in the active layer of P3HT:PCBM. The area under the absorption peak shows the light harvesting ability of photoactive layer [20]. In ternary blend, the absorption area enhanced from visible light to near infrared zone. The absorption enhanced with increasing amount of CuO nanoparticles in the active layer.

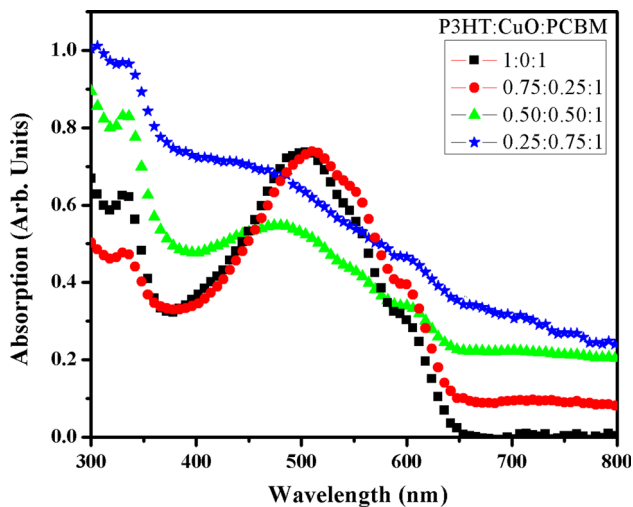


Fig. 6 UV-Vis absorption spectra of various ratios of P3HT:CuO:PCBM active layer

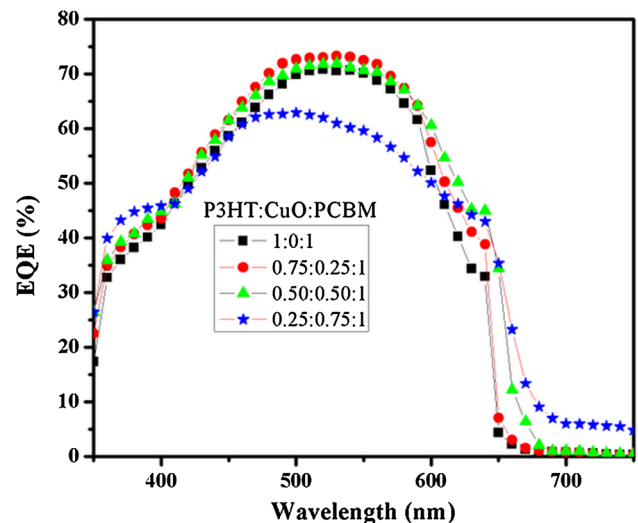


Fig. 8 EQE curves of various ratios of inverted hybrid solar cells

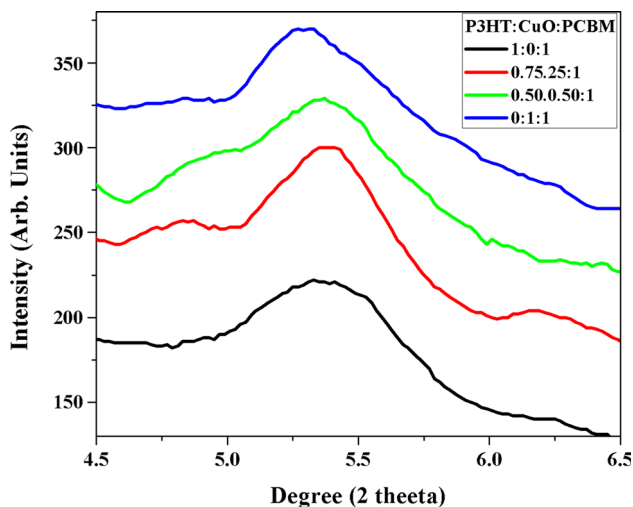


Fig. 7 XRD results of various blends of P3HT:CuO:PCBM in DCB, showing a trend of increased crystallinity of the P3HT

As revealed above, the roughness improved with an increasing amounts of nanoparticles in the active layer. High rough surface might lead to increase absorption due to increased light reflecting in the active layer [3, 21].

The incorporation of CuO to the P3HT:PCBM polymer blend also observed to increase the P3HT crystallinity gradually as supported by XRD results (Fig. 7). Various groups reported that the incorporation of small amounts of inorganic semiconductor nanoparticles could enhance the crystallinity of P3HT [13]. This increase in crystallinity of the P3HT region appears to be partially responsible for the increase in the absorption and PCE of the devices.

The EQE curves of various ratios of P3HT:CuO:PCBM solar cells are shown in Fig. 8. Figure 8 indicates that the

EQE increased with incorporation of CuO in the active layer of P3HT:PCBM solar cells. This improvement in EQE over 400–600 nm wavelength zone contributes to the increase in PCE of the ternary blend. This enhancement in EQE is attributed to increase in absorption and charge mobility of the active layer of the devices [12, 13].

4 Conclusion

Inverted structure hybrid BHJ solar cells were fabricated and based on a ternary system of P3HT, CuO and PCBM nanoparticles were studied. The devices incorporated CuO nanoparticles showed better performance as compared with the control device (P3HT:PCBM). The replacement of P3HT with CuO enhanced the PCE from a baseline of ~ 3.4 to 3.7 % in DCB upon addition of the optimum amount of CuO nanoparticles in the active layer. The improved efficiency was mostly due to increase in V_{oc} , J_{sc} and increase in the absorbance. The mixing of CuO in the active layer introduced red shift and enhanced the absorbance light range with increasing amount of CuO in the P3HT:PCBM blend. The crystallinity of P3HT increased with increasing amount of CuO in the active layer blend. The mixing of CuO nanoparticles also increased the EQE of the devices. The CuO nanoparticles aggregated with increasing amount of CuO in the active layer and enhanced the surface roughness. The CuO nanoparticles agglomerated as their concentration increased relative to PCBM.

Acknowledgments The author would like to acknowledge the financial support of higher education commission (HEC) Pakistan for 6 month scholar (IRSIP) in Queen's University Canada.

References

1. B.V.K. Naidu, J.S. Park, S.C. Kim, S.-M. Park, E.-J. Lee, K.-J. Yoon, S.J. Lee, J.W. Lee, Y.-S. Gal, S.-H. Jin, *Sol. Energy Mater. Sol. Cells* **92**, 397 (2008)
2. A.J. Morfa, K.L. Rowlen, T.H. Reilly, M.J. Romero, J. van de Lagemaat, *Appl. Phys. Lett.* **92**, 13504 (2008)
3. M. Park, B.D. Chin, J.-W. Yu, M.-S. Chun, S.-H. Han, *J. Ind. Eng. Chem.* **14**, 382 (2008)
4. T. Ameri, P. Khoram, J. Min, C.J. Brabec, *Adv. Mater. (Deerfield Beach, FL)* **25**, 4245 (2013)
5. Y.-C. Chen, C.-Y. Hsu, R.Y.-Y. Lin, K.-C. Ho, J.T. Lin, *ChemSusChem* **6**, 20 (2013)
6. L. Yang, L. Yan, W. You, *J. Phys. Chem. Lett.* **4**, 1802 (2013)
7. S. Honda, T. Nogami, H. Ohkita, H. Benten, S. Ito, *ACS Appl. Mater. Interfaces* **1**, 804 (2009)
8. S. Honda, H. Ohkita, H. Benten, S. Ito, *Chem. Commun. (Camb.)* **46**, 6596 (2010)
9. S. Honda, H. Ohkita, H. Benten, S. Ito, *Adv. Energy Mater.* **1**, 588 (2011)
10. S. Honda, S. Yokoya, H. Ohkita, H. Benten, S. Ito, *J. Phys. Chem. C* **115**, 11306 (2011)
11. H. Xu, T. Wada, H. Ohkita, H. Benten, S. Ito, *Electrochim. Acta* **100**, 214 (2013)
12. M. Ikram, S. Ali, R. Murray, A. Hussain, I. U-din, S.I. Shah, *Curr. Appl. Phys.* **15**, 48 (2015)
13. M. Ikram, R. Murray, A. Hussain, S. Ali, S.I. Shah, *Mater. Sci. Eng. B* **189**, 64 (2014)
14. A. Mittiga, E. Salza, F. Sarto, M. Tucci, R. Vasanthi, *Appl. Phys. Lett.* **88**, 163502 (2006)
15. M. Jørgensen, K. Norrman, F.C. Krebs, *Sol. Energy Mater. Sol. Cells* **92**, 686 (2008)
16. W.-H. Baek, I. Seo, T.-S. Yoon, H.H. Lee, C.M. Yun, Y.-S. Kim, *Sol. Energy Mater. Sol. Cells* **93**, 1587 (2009)
17. W. Shockley, H.J. Queisser, *J. Appl. Phys.* **32**, 510 (1961)
18. N. Sekine, C.-H. Chou, W.L. Kwan, Y. Yang, *Org. Electron.* **10**, 1473 (2009)
19. Y.-F. Lim, J.J. Choi, T. Hanrath, *J. Nanomater.* **2012**, 1 (2012)
20. H. Fu, M. Choi, W. Luan, Y.-S. Kim, S.-T. Tu, *Solid-State Electron.* **69**, 50 (2012)
21. S.H. Oh, S.J. Heo, J.S. Yang, H.J. Kim, *ACS Appl. Mater. Interfaces* **5**, 11530 (2013)